Anomaly Detection of Subsurface Objects Using Handheld Ground-Penetrating Radar

K.C. Ho, Samuel Harris, Alina Zare, Matthew Cook
Department of Electrical and Computer Engineering, University of Missouri, Columba, MO USA 65211

ABSTRACT

This paper develops an anomaly detection algorithm for subsurface object detection using the handheld ground penetrating radar. The algorithm is based on the Mahalanobis distance measure with adaptive update of the background statistics. It processes the data sequentially for each data sample in a causal manner to generate detection confidences. The algorithm is applied to process the data from two different radars, an impulse and a step-frequency, for performance evaluation.

Keywords: Ground penetrating radar, Mahalanobis distance, signal processing, subsurface object detection

1. INTRODUCTION

Landmines and other buried explosives endanger the lives of people worldwide. These hazards are usually placed during times of war and claim the lives of numerous soldiers each year. In addition, landmines sometimes remain buried long after hostilities have ended and render large regions of land unsafe for civilian activity. The threat posed by these underground weapons has motivated the research and development of various kinds of subsurface object detectors.

The goal of subsurface object detection is to create systems that are capable of safely locating and accurately identifying different types of buried targets. Such detectors typically utilize one or more physical sensors in order to attain a digital representation of an underground area. This data is then analyzed by several algorithms in order to determine if a landmine or other type of explosive is present.

Electromagnetic induction sensors, commonly referred to as metal detectors, have long been used for subsurface object detection. However, these sensors are only effective at locating objects with high metal content and many modern explosives contain little or no metal. It has been shown that ground penetrating radar (GPR) can be used to identify these targets.

Two popular platforms for GPR in subsurface object detection are vehicle mounted and hand-held. The vehicle mounted platform focuses on the detection of anti-tank targets and performs the detection in a relatively fast pace by driving down a road. The hand-held system, on the other hand, requires an operator to sweep the detector back and forth over the ground while moving forward and the detection is a relatively slow pace. The main advantage of the hand-held system is that it can operate in different terrain.

There are a number of popular hand-held detection systems, including the AN/PSS-14[1-2] and the Mine Hound[3]. The former uses a step-frequency GPR whilst the latter a pulse GPR. In addition to GPR, both contain the EMI sensor as well to improve the detection for anti-personnel targets.

Due to the improvement of technology, better hand-held GPRs may be available to improve the hand-held detector performance. In this paper, we shall revisit the signal processing algorithm and propose an anomaly detector that can act as a prescreener to identify alarm locations that potentially contain targets, so that more sophisticated algorithms[4-6] can be applied there to ascertain if targets are present.

This paper is organized as follows. The next section describes the hand-held GPR data. Section 3 presents the proposed anomaly detection algorithm. Section 4 gives experimental results and evaluates the performance of the proposed algorithm using data collected at a government test site. Section 5 concludes the paper.

Distribution Statement A: Approved for public release: distribution is unlimited

Detection and Sensing of Mines, Explosive Objects, and Obscured Targets XX,
edited by Steven S. Bishop, Jason C. Isaacs, Proc. of SPIE Vol. 9454, 94541B
© 2015 SPIE · CCC code: 0277-786X/15/$18 · doi: 10.1117/12.2178584

Downloaded From: http://proceedings.spiedigitallibrary.org/ on 05/27/2015 Terms of Use: http://spiedl.org/terms

2. DATA DESCRIPTION

The GPR used in this study is an impulse radar, which sends out a wideband pulse that propagates into the ground. At each location, the returned signal is measured by three spatially separated receivers on the unit. The hand-held detector is carried by a robot. The arm of the robot sweeps the detector back and forth while moving forward, providing a sequence of GPR data for processing.

The data is collected at a constant sampling rate in time and it does not have constant spatial separation between two successive samples due to the non-uniform sweeping speed where the speed reduces at the end of each cross-track sweep[7]. In the processing described below, the data are downsampled to a constant spatial sampling of 1 cm/sample. We shall represent the spatially regulated data, which are real, as $x_c(i, j)$, where c denotes the channel number, i the depth index and j the sample index. For convenience purpose we also denote the data as a 2-D matrix $\mathbf{X}_c = [\mathbf{x}_c(1), \mathbf{x}_c(2), \ldots]$, where $\mathbf{x}_c(j)$ is a column vector of length 256 that designates the collection of the data values along depth at sample j. The proposed anomaly detection algorithm processes each channel independently.

3. PROCESSING ALGORITHM

3.1 Ground alignment

Due to the roughness of the ground and the mechanical vibration of the robot arm caused by movement, the ground level shown in the acquired data is drifted up and down. The first step in the processing is to align the data from one sample to the next so that the ground level at each sample appears at the same depth bin. Each sample refers to a vector that consists of 256 points.

Ground alignment uses cross-correlation to determine the translation between the current and the reference sample. The reference sample is obtained by the average of the first few samples. The ground of the reference sample is placed such that its minimum value appears at depth bin 25. Each data sample is correlated with the reference to determine the relative shift so that it aligns with the reference. Fig. 1 shows an example of the data before and after the alignment. It clearly illustrates the effectiveness of the alignment method.

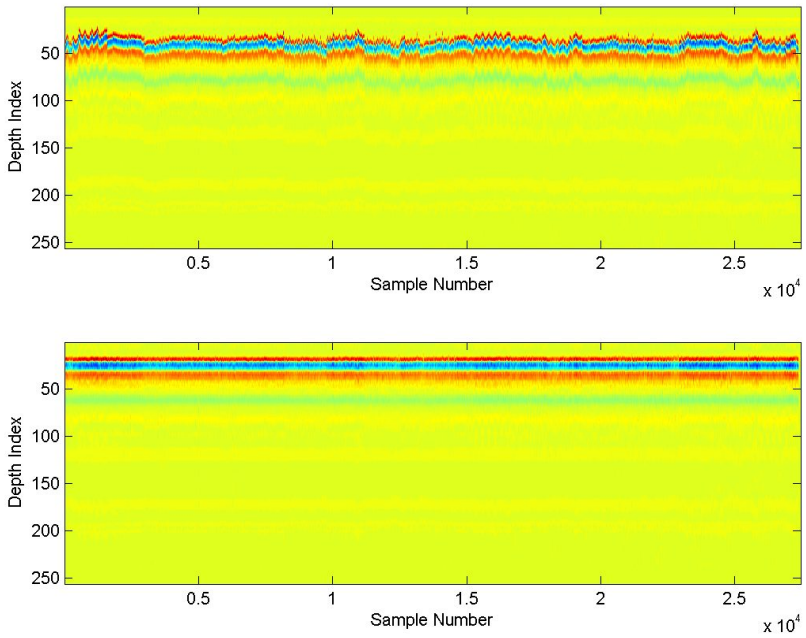

Fig. 1 Data before (top) and after (bottom) ground alignment

Downloaded From: http://proceedings.spiedigitallibrary.org/ on 05/27/2015 Terms of Use: http://spiedl.org/terms

3.2 Background removal

The background consists of the self-signature of the radar and the radar return from bare soil. The background can be very strong such that it can dominate the radar return. This can occur even when a target appears whose response is super-imposed in the overall return. The background is non-stationary and varies dynamically. We model the background response in the current sample by a weighted sum of the past few samples,

$$\mathbf{b}(j) = \sum_{l=P}^{P+L-1} a_l(j)\mathbf{x}(j-l) \tag{1}$$

where $\mathbf{b}(j)$ is a column vector that represents the background estimate at sample j, P is the number of guard samples, L is the number of samples used to estimate the background, $a_l(j)$ is the weighting coefficient and $\mathbf{x}(j)$ is the j-th sample of the data. The subscript c that indicates the channel is dropped for notation simplicity. In the current processing, we set P to five and L to unity.

The background-removed sample is obtained by

$$\mathbf{y}(j) = \mathbf{x}(j) - \mathbf{b}(j)\,. \tag{2}$$

To take into account the dynamic variation of the background, the weighting coefficient $a_l(j)$ is estimated by minimizing the L_2 norm of $\mathbf{y}(j)$:

$$a_P(j) = \frac{\mathbf{x}^T(j)\mathbf{x}(j-P)}{\mathbf{x}^T(j-P)\mathbf{x}(j-P)}\,.$$

Fig. 2 depicts the data before and after background removal. The data is much cleaner after removing the background.

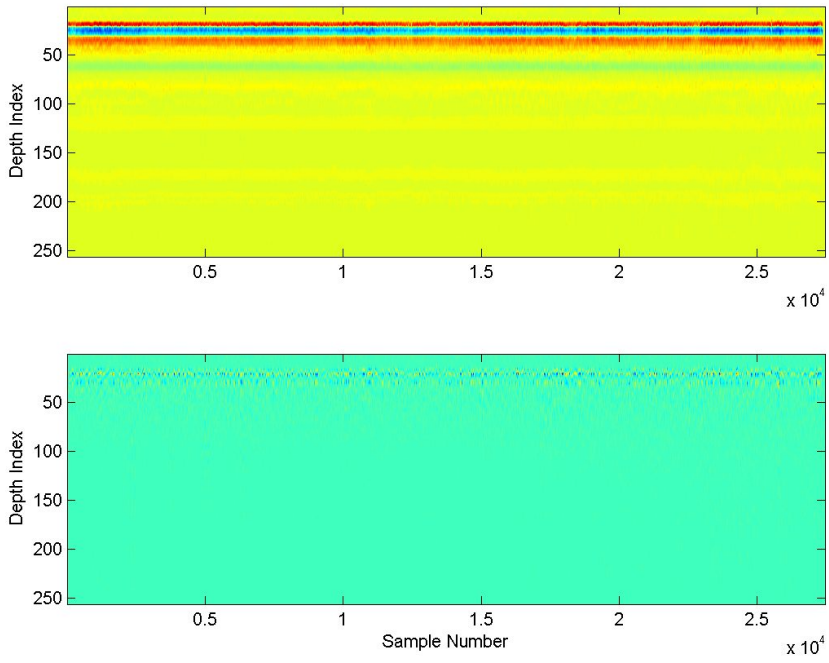

Fig. 2 Data before (top) and after (bottom) background removal

Downloaded From: http://proceedings.spiedigitallibrary.org/ on 05/27/2015 Terms of Use: http://spiedl.org/terms

3.3 Detection statistic

The detection statistic is generated using the Mahalanobis distance[8]. Assuming $\mathbf{y}(j\text{-}1)$ is a background sample, the running mean and the running covariance matrix for the current sample $\mathbf{y}(j)$ are obtained by

$$\mathbf{m}(j) = \lambda \mathbf{m}(j-1) + (1-\lambda)\mathbf{y}(j-1) \tag{3}$$

$$\mathbf{C}(j) = \lambda \mathbf{C}(j-1) + (1-\lambda)\,(\mathbf{y}(j-1) - \mathbf{m}(j-1))^T\,(\mathbf{y}(j-1) - \mathbf{m}(j-1)). \tag{4}$$

The smoothing constant λ is set to 0.999.

The detection statistic is

$$f(j) = (\mathbf{y}(j) - \mathbf{m}(j))^T\,\mathbf{W}(j)(\mathbf{y}(j) - \mathbf{m}(j)).$$

The matrix $\mathbf{W}(j)$ is the inverse of the running covariance of $\mathbf{C}(j)$. To reduce computation, we apply the Woodbury matrix identity[9] to update $\mathbf{W}(j)$ directly,

$$\mathbf{W}(j) = \frac{1}{1-\lambda}\left(\mathbf{W}(j-1) - \frac{\mathbf{W}(j-1)(\mathbf{y}(j-1) - \mathbf{m}(j-1))\,(\mathbf{y}(j-1) - \mathbf{m}(j-1))^T\,\mathbf{W}(j-1)}{(1-\lambda)/\lambda + (\mathbf{y}(j-1) - \mathbf{m}(j-1))^T\,\mathbf{W}(j-1)(\mathbf{y}(j-1) - \mathbf{m}(j-1))}\right) \tag{5}$$

For the next sample, we update the running mean $\mathbf{m}(j+1)$ and covariance inverse $\mathbf{W}(j+1)$ using (3) and (5) if the detection statistic $f(j)$ is less than a certain threshold, which indicates $\mathbf{y}(j)$ is considered as a background sample. Otherwise, we simply set $\mathbf{m}(j+1)$ to $\mathbf{m}(j)$ and $\mathbf{W}(j+1)$ to $\mathbf{W}(j)$, without updating the background statistics.

3.4 Range gating and depth segmentation

To improve performance, we apply range gating to process the data below the ground bounce only. Furthermore, we separate the data into two depth regions evenly, shallow and deep, with slight overlap. The detection statistics are generated separately for the two depth segments. The final detection statistic is the maximum of the two.

4. EXPERIMENTAL RESULTS

The data for performance evaluation were collected in March of 2014, using the robot mounted hand-held GPR system described in Section 2. The dataset contains twelve lanes with one run in each. Each lane contains a variety of targets, including anti-personnel (AP), anti-tank (AT) and wire, with high, low and no metal content. We shall illustrate the performance in terms of the Receiver Operating Characteristics (ROC) curves.

The data have three channels and the proposed algorithm in Section 3 was applied to each channel separately. The detection values of the three channels were merged together into a single surface map for scoring. The ground truth locations with 0.25 m halo size are overlaid in a surface map to generate the correct detections and false alarms. Fig. 3 shows the surface detection map of one lane. The targets are buried in the middle of the lane at regular spacing.

Fig. 4 gives the ROC curve for all targets, where the shaded area denotes the 90% confidence interval of detection at a given false alarm rate. Also shown is the performance of the energy detector after range gating to remove the ground bounce. The proposed algorithm works much better than the energy detector. There are a number of anti-personnel targets that are very difficult to detect by the GPR.

Fig. 5 shows the performance when we do not count the anti-personnel targets and wires. The results are much better compared to Fig. 3, and we are able to reach 90% detection at a false alarm rate of $0.15/m^2$.

Downloaded From: http://proceedings.spiedigitallibrary.org/ on 05/27/2015 Terms of Use: http://spiedl.org/terms

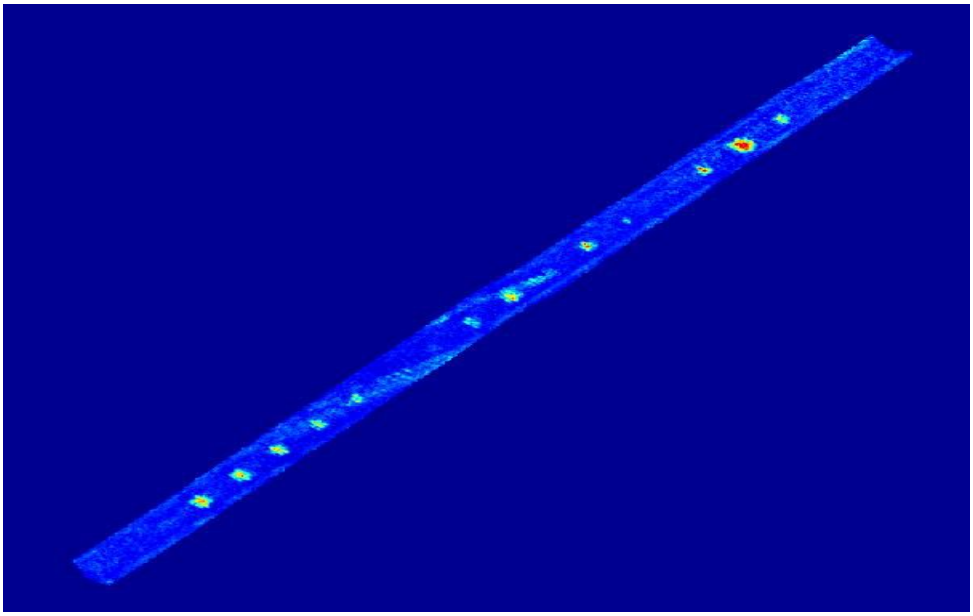

Fig. 3 The surface detection map produced by the proposed algorithm at a certain lane

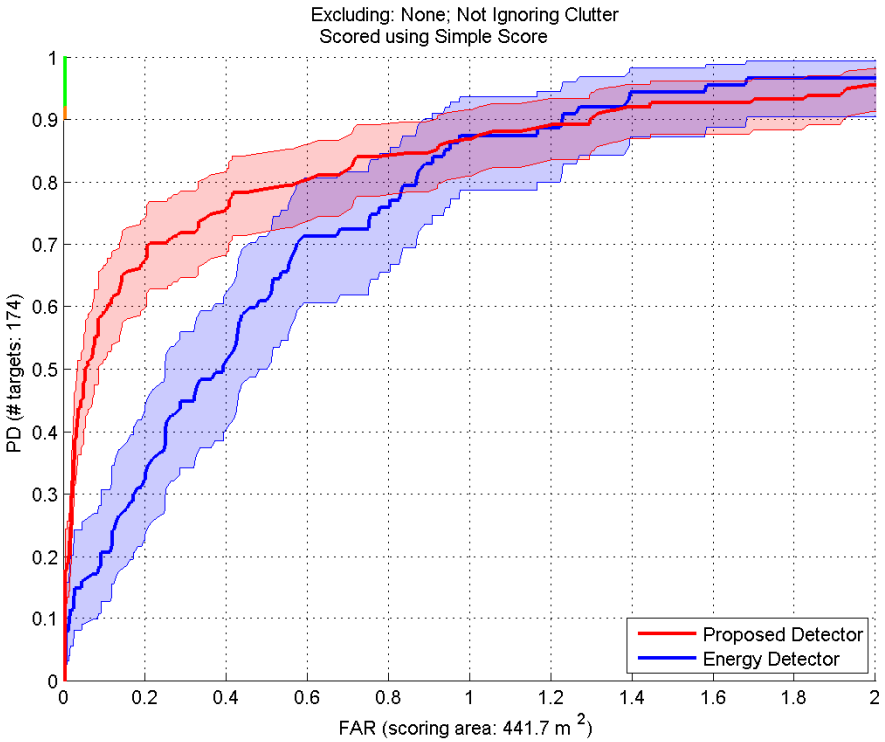

Fig. 4 Detection performance of all targets including AP, AT and wires of various metal content

Downloaded From: http://proceedings.spiedigitallibrary.org/ on 05/27/2015 Terms of Use: http://spiedl.org/terms

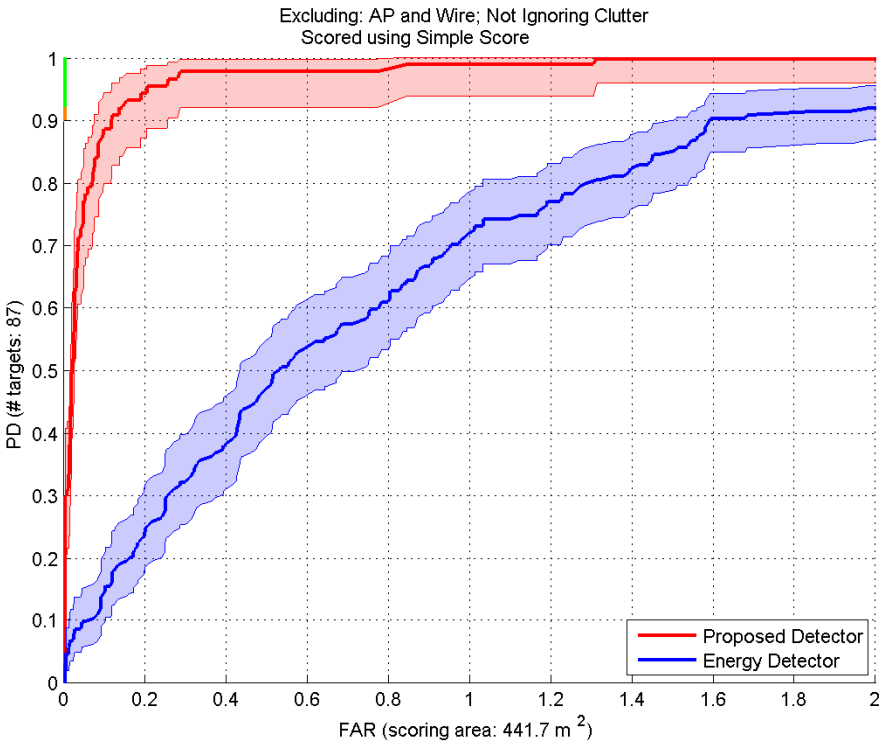

Fig. 5 Detection performance without counting AP and wires

5. CONCLUSION

We have proposed an anomaly detector for the hand-held GPR system. It can act as a pre-screener to identify alarm locations that potentially contain a target, where more sophisticated algorithms can be applied to improve the detection performance. The proposed detector consists of ground alignment, background removal, depth segmentation and Mahalanobis distance computation. The performance of the proposed detector outperforms the energy detector significantly.

ACKNOWLEDGMENT

This work was funded by Army Research Office grant number 66398-CS to support the US Army RDECOM CERDEC NVESD.

REFERENCES

[1] K. C. Ho and P. D. Gader, "An Improved Correlation Based Detector for Hand-held Landmine Detector," in *Proc. SPIE Conf. Detection and Remediation Technologies for Mines and Minelike Targets VI*, Orlando, Apr. 2001.

[2] P. Ngan, S. Burke, R. Cresci, J. N. Wilson, P. D. Gader, K. C. Ho, E. E. Bartosz, and H. A. Duvoisin, *"*Development of region processing algorithm for HSTAMIDS: status and field test results,*" in Proc. SPIE Conf. Detection and Remediation Technologies for Mines and Minelike Targets XII,* Orlando, Apr. 2007.

Downloaded From: http://proceedings.spiedigitallibrary.org/ on 05/27/2015 Terms of Use: http://spiedl.org/terms

[3] D. Daniels, J. Braunstein, and M. Nevard, "Using minehound in Cambodia and Afghanistan," *J. ERW Mine Action*, pp. 46-50, 2014.
[4] K. C. Ho, P. D. Gader, and J. B. Devaney, "Locate mode processing for hand held land mine detector," in *Proc. SPIE Conf. Detection and Remediation Technologies for Mines and Minelike Targets VII*, Orlando, Apr. 2002.
[5] J. N. Wilson, P. D. Gader, K. C. Ho, W. H. Lee, J. R. Stanley, and T. C. Glenn, "Region processing of ground penetrating radar and electromagnetic induction for handheld landmine detection," in *Proc. SPIE Conf. Detection and Remediation Technologies for Mines and Minelike Targets IX*, Orlando, Apr. 2004.
[6] P. Ngan, S. Burke, R. Cresci, J. N. Wilson, K. C. Ho, and P. D. Gader, *"Region processing algorithm for HSTAMIDS," in Proc. SPIE Conf. Detection and Remediation Technologies for Mines and Minelike Targets XI*, Orlando, Mar. 2006.
[7] J. N. Wilson, K. C. Ho, and P. D. Gader, "An analysis of sweep patterns for handheld demining system," *in Proc. SPIE Conf. Detection and Remediation Technologies for Mines and Minelike Targets XI*, Orlando, Mar. 2006.
[8] C. M. Bishop, *Pattern Recognition and Machine Learning.* Springer, 2006.
[9] S. M. Kay, *Fundamentals of Statistical Signal Processing: Estimation Theory*, Prentice Hall, 1993.

Downloaded From: http://proceedings.spiedigitallibrary.org/ on 05/27/2015 Terms of Use: http://spiedl.org/terms